AGU PUBLICATIONS

Geophysical Research Letters

RESEARCH LETTER
10.1002/2017GL073529

Special Section:
Early Results: Juno at Jupiter

Independent evolution of stratospheric temperatures in Jupiter's northern and southern auroral regions from 2014 to 2016

J. A. Sinclair[1], G. S. Orton[1], T. K. Greathouse[2], L. N. Fletcher[3], C. Tao[4], G. R. Gladstone[2], A. Adriani[5], W. Dunn[6], J. I. Moses[7], V. Hue[2], P. G. J. Irwin[8], H. Melin[3], and R. S. Giles[8]

[1] Jet Propulsion Laboratory, California Institute of Technology, Pasadena, California, USA, [2] Southwest Research Institute, San Antonio, Texas, USA, [3] Department of Physics and Astronomy, University of Leicester, Leicester, UK, [4] Space Environment Laboratory, National Institute of Information and Communications Technology, Tokyo, Japan, [5] Institute for Space Astrophysics and Planetology, Rome, Italy, [6] Mullard Space Science Laboratory, University College London, London, UK, [7] Space Science Institute, Boulder, Colorado, USA, [8] Atmospheric, Oceanic and Planetary Physics, University of Oxford, Oxford, UK

Key Points:
- Stratospheric temperatures in Jupiter's northern and southern auroral regions evolve independently
- The 1 mbar temperature in Jupiter's northern auroral region exhibited a net negligible change from 2014 to 2016
- The 1 mbar temperature in Jupiter's southern auroral region exhibited a net increase of over 10 K from 2014 to 2016

Correspondence to:
J. A. Sinclair,
james.sinclair@jpl.nasa.gov

Citation:
Sinclair, J. A., et al. (2017), Independent evolution of stratospheric temperatures in Jupiter's northern and southern auroral regions from 2014 to 2016, *Geophys. Res. Lett.*, *44*, 5345–5354, doi:10.1002/2017GL073529.

Received 6 APR 2017
Accepted 25 MAY 2017
Accepted article online 30 MAY 2017
Published online 12 JUN 2017

Abstract We present retrievals of the vertical temperature profile of Jupiter's high latitudes from Infrared Telescope Facility-Texas Echelon Cross Echelle Spectrograph measurements acquired on 10–11 December 2014 and 30 April to 1 May 2016. Over this time range, 1 mbar temperature in Jupiter's northern and southern auroral regions exhibited independent evolution. The northern auroral hot spot exhibited negligible net change in temperature at 1 mbar and its longitudinal position remained fixed at 180°W (System III), whereas the southern auroral hot spot exhibited a net increase in temperature of 11.1 ± 5.2 K at 0.98 mbar and its longitudinal orientation moved west by approximately 30°. This southern auroral stratospheric temperature increase might be related to (1) near-contemporaneous brightening of the southern auroral ultraviolet/near-infrared H_3^+ emission measured by the Juno spacecraft and (2) an increase in the solar dynamical pressure in the preceding 3 days. We therefore suggest that 1 mbar temperature in the southern auroral region might be modified by higher-energy charged particle precipitation.

1. Introduction

Auroral emissions are the process through which the interaction of a planet's atmosphere and its external magnetosphere can be studied. Jupiter exhibits auroral emission over much of the electromagnetic spectrum as a result of charged particle precipitation and energy deposition in the upper atmosphere [e.g., *Gladstone et al.*, 2002; *Nichols et al.*, 2007; *Ozak et al.*, 2010; *Stallard et al.*, 2012; *Giles et al.*, 2016]. Enhanced stratospheric midinfrared emission of CH_4, C_2H_2, C_2H_4, and C_2H_6 [*Caldwell et al.*, 1980; *Kim et al.*, 1985; *Drossart et al.*, 1986; *Kostiuk et al.*, 1993; *Livengood et al.*, 1993; *Drossart et al.*, 1993; *Flasar et al.*, 2004a] is also observed in locations coincident with Jupiter's shorter-wavelength auroral emission (~70°N, 180°W (planetographic, System III) and 72°S, 330–80°W). This *auroral-related* emission provides evidence that a significant amount of auroral energy is also imparted as deep as Jupiter's stratosphere ($p > 1$ μbar) leading to elevated temperatures.

The mechanism for this phenomenon is, however, not well understood. A recent retrieval analysis in *Sinclair et al.* [2017] of infrared spectra measured by Voyager and Cassini indicated that stratospheric temperatures in auroral regions are predominantly heated in two discrete pressure levels: the first at approximately 1 mbar level and the second at 10 μbar level (and lower pressures where the midinfrared observations have no sensitivity). Temperatures at 10 μbar level are considered to be a direct influence of the energetic particle precipitation, varying on timescales as short as days [*Kostiuk et al.*, 1993; *Romani et al.*, 2008]. However, we suggested several possible mechanisms for the source of 1 mbar heating including the presence of aurorally produced haze particles [*Gladstone et al.*, 2002; *Wong et al.*, 2000; *Friedson et al.*, 2002] which are heated by UV/visible radiation or the precipitation of a higher-energy population of charged particles.

In July 2016, the Juno spacecraft [*Bolton and Juno Science Team*, 2006, 2016] performed its orbital insertion around Jupiter and has since begun a 53.5 day cadence of measurements performed during close flybys

or *perijoves*. Juno's science payload was designed to provide a powerful understanding of the interaction of Jupiter's external magnetosphere with its upper atmosphere. In addition, the science return of Juno will be greatly enhanced by a supporting Earth-based observing campaign covering a large range in wavelengths. In particular, Earth-based midinfrared (5–15 μm) observations form an important component of this supporting campaign since Juno's science payload does not contain an instrument that operates in this spectral range.

In this work, we present temperature retrievals of IRTF-TEXES (Infrared Telescope Facility-Texas Echelon Cross Echelle Spectrograph [*Lacy et al.*, 2002] on NASA's Infrared Telescope Facility) observations measured in December 2014 and April 2016. These results will be compared to assess the evolution of stratospheric temperatures in Jupiter's auroral regions. The magnitude, altitude, and timescales over which temperatures vary in the auroral regions will be used to test the aforementioned hypotheses of the mechanisms driving the auroral-related stratospheric heating. In addition, these results will serve as a baseline context during the approach of the Juno spacecraft, with which future TEXES measurements can be compared. Such future measurements will allow the variability of Jupiter's auroral-related stratospheric heating to be assessed on shorter timescales and will extend the time series to periods contemporaneous with Juno measurements and the extensive ground-based campaign. Near-simultaneous measurements of 1 mbar temperature in the auroral regions, the shorter-wavelength auroral emission and the external magnetospheric conditions will serve as a powerful tool in determining exactly how the lower stratosphere is coupled to the magnetosphere.

2. Observations and Analysis

2.1. IRTF-TEXES Observations

TEXES is a cryogenic grating spectrometer that measures spatially resolved spectra in the mid-to-far infrared (5–25 μm) at high spectral resolving powers [*Lacy et al.*, 2002]. Using TEXES on NASA's Infrared Telescope Facility (IRTF) on 10–11 December 2014 and 30 April to 1 May 2016, high-resolution $R = 60,000–85,000$ spectra were obtained of Jupiter's high latitudes. The absolute relative velocities of Earth and Jupiter during these observations were approximately 23 km/s, which allowed telluric and Jovian CH_4 features to be disentangled. The slit (9–19 arc sec in length and 1.4 or 2 arc sec in width, depending on the spectral setting) was orientated parallel to Jupiter's central meridian. Starting from dark sky west of high northern latitudes, the slit was stepped east in increments of 0.7 arc sec perpendicular to the slit length until dark sky east of the planet, providing longitudinally resolved spectra poleward of 45°N and dark sky for subtraction and noise calculations. Spectra were obtained in five discrete settings each with a range of 4–6 cm^{-1} centered on wave numbers of 587, 730, 819, 950, and 1248 cm^{-1}, which, respectively, captured emission of H_2 S(1), C_2H_2, C_2H_6, C_2H_4, and CH_4. In December 2014, 587 cm^{-1} spectra were measured at a resolution of 6 km/s (or 0.012 cm^{-1}), while all other settings were measured at 4 km/s (0.0097 to 0.017 cm^{-1} depending on the setting). In April 2016, a motor driver failure meant that all spectra were measured at a resolution of 4 km/s.

The slit was then moved to Jupiter's southern hemisphere, and similar scans were obtained of high southern latitudes. The wavelength-dependent noise in each spectral setting was calculated as the standard deviation in all sky pixels. This resulted in higher noise values in regions of high telluric absorption, which ensured that these spectral regions were weighted less in subsequent retrievals (section 2.2). These north-south scan pairs in all five spectral settings were repeated over time such that Jupiter's rotation allowed the longitudinal coverage to be extended. In December 2014, we obtained longitudinal coverage from approximately to 0° to 270°W (System III) and in April 2016 from 60° to 360°W. In each spectral setting, individual spectra were coadded into spatial bins. Spatial bins were 4° wide in planetographic latitude and stepped in increments of 2° and 20° in System III longitude and stepped in 10° increments to obtain Nyquist sampling. The resulting noise of the coadded spectra was calculated to be the larger of either (1) the noise on the individual spectra combined in quadrature or (2) the standard deviation of the mean.

2.2. Temperature Retrievals

The vertical temperature profile was retrieved from the H_2 S(1) and CH_4 emission spectra. The vertical profiles of H_2 and CH_4 were assumed to be horizontally homogenous below their homopause [*Moses et al.*, 2005]: spatial variations in their emission were assumed to arise from temperature changes alone. The following wave number ranges were adopted in the retrieval of temperature from TEXES observations in 2014 in order to capture H_2 S(1) emission, a mixture of weak and strong CH_4 lines, while avoiding the following gaps in spectral coverage: 587.0–587.1, 1245.18–1246.55, 1245.74–1246.0, 1246.45–1246.90, 1247.82–1249.0, and 1249.6–1250.3 cm^{-1}. For retrievals of 2016 TEXES observations, the following wave number ranges

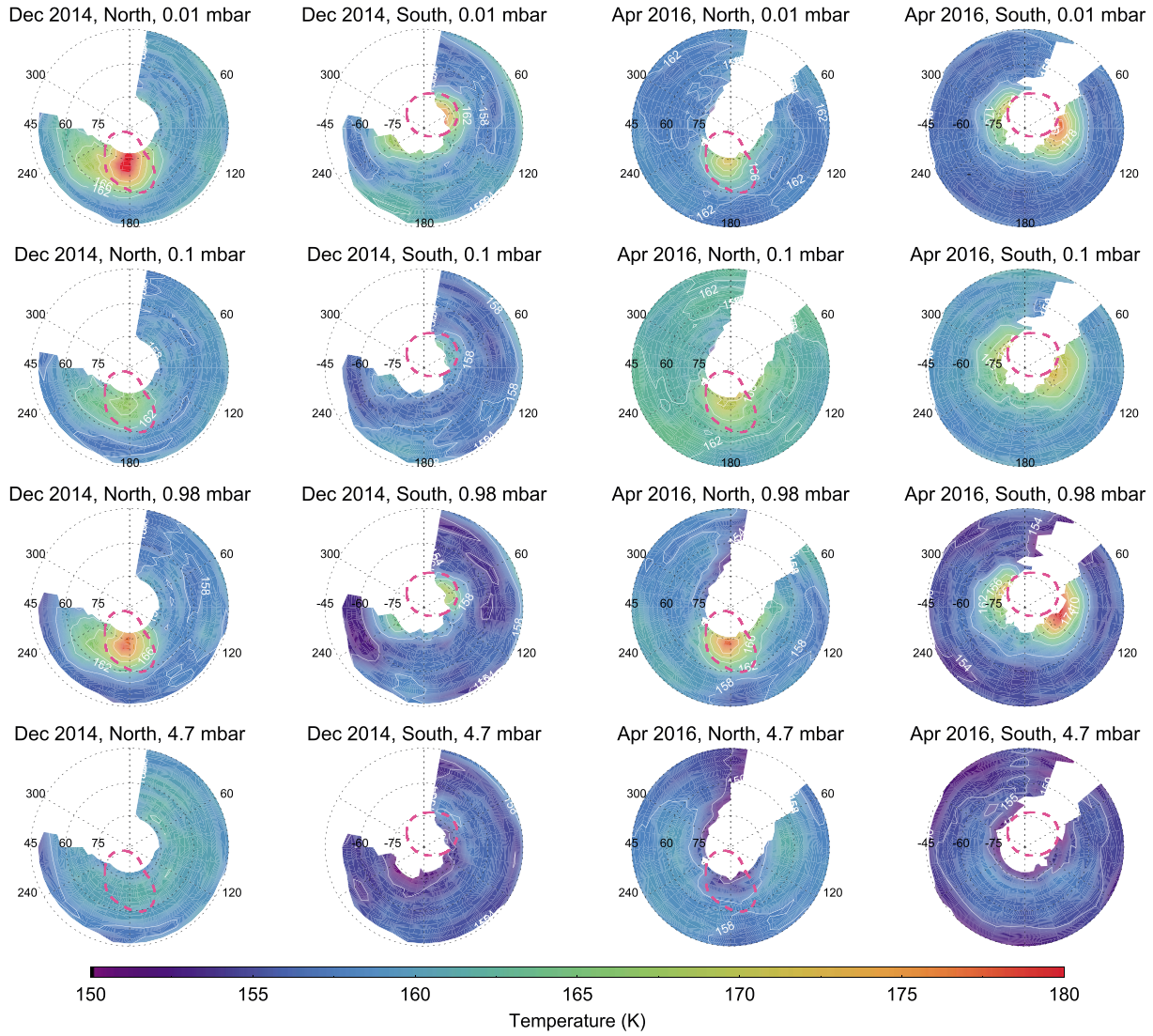

Figure 1. Retrieved temperature distributions at Jupiter's high northern and southern latitudes (first and second columns) on 10–11 December 2014 and (third and fourth columns) 30 April to 1 May 2016. Results are shown at 0.01 mbar (first row), 0.1 mbar (second row), 0.98 mbar (third row), and 4.7 mbar (fourth row). The color-temperature conversion is indicated in the color bar at the bottom and white contour lines represent temperature increments of 5 K. Pink dashed lines represent the mean position of the auroral ovals in February 2007 and June 2007, which is believed to capture the range in the position of the ultraviolet oval in time [*Bonfond et al.*, 2012].

were adopted: 587.0–587.1, 1245.0–1245.225, 1245.5–1245.76, 1246.2–1246.49, 1247.6–1247.75, and 1249.4–1249.67 cm^{-1}. The differing spectral coverage of the TEXES observations in December 2014 and April 2016 resulted from the contrasting relative velocities of Jupiter with respect to Earth (~ -23 km/s and +23 km/s, respectively), which resulted in different portions of the CH_4 lines being observable with respect to regions of high telluric absorption.

Retrievals were performed using NEMESIS [*Irwin et al.*, 2008], a forward model and retrieval tool. The a priori temperature profile detailed in *Sinclair et al.* [2017] was also adopted as the a priori profile in this work. However, several alternative temperatures a priori were also tested to determine the robustness of retrieved profiles with respect to initial assumptions. We will present retrievals of the vertical profiles of C_2H_2, C_2H_4, and C_2H_6 and their evolution from 2014 to 2016 in future work.

3. Thermal Structure in April 2016

Figure 1 shows the retrieved temperature distributions at high northern and high southern latitudes in December 2014 and April 2016. We first discuss features of the thermal structure in April 2016, during the

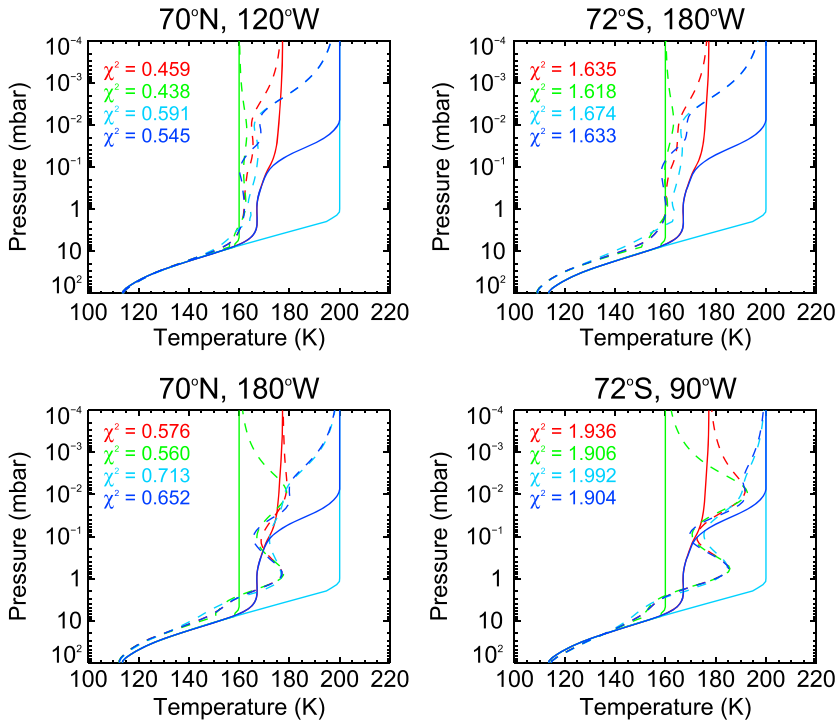

Figure 2. Test temperature retrievals using different a priori at 70°N, 120°W (top-left, a representative quiescent location), 70°N, 180°W (bottom-left, the northern auroral hot spot), 72°S, 180°W (top-right, a representative quiescent location in the south), and 72°S, 90°W (bottom-right, the position of the southern auroral hot spot). A priori profiles are shown as solid lines, and the corresponding retrievals are shown as dashed lines of the same color. The χ^2/n values of each retrieval are also shown to quantify how well the modelled spectra fit the observed spectra. The best fitting spectra are shown in Figure 3.

approach of the Juno spacecraft and will discuss the inferred evolution in comparing December 2014 and April 2016 results in section 4.

In both auroral regions, we find that there is no evidence of auroral-related heating at the 5 mbar level: we believe that 1–5 mbar range marks the highest pressure at which auroral energy can modify the thermal structure. This is also consistent with the findings of Composite Infrared Spectrometer (CIRS) measurements [*Flasar et al.*, 2004b; *Sinclair et al.*, 2017]. Over 1 mbar to 10 μbar pressure range, there is evidence of elevated temperatures in locations coincident with the ultraviolet auroral oval features [*Bonfond et al.*, 2012]. However, within this pressure range, we find that stratospheric temperatures are predominantly elevated at 1 mbar and 10 μbar pressure levels, with comparably less heating at the intermediate 0.1 mbar level. These results are consistent with our analysis of Cassini-CIRS observations obtained of Jupiter in 2001 [*Sinclair et al.*, 2017] as well as a recent analysis by *Kostiuk et al.* [2016].

This bifurcation of the vertical temperature profile in the auroral hot spots is further demonstrated in Figure 2. In both the northern and southern auroral regions, the temperature profile reaches a maximum at ~1 mbar, subsequently decreases to a minimum at 0.1 mbar, and subsequently increases to 10 μbar level. This result is consistent regardless of the chosen temperature a priori profile, even when a significantly cooler or warmer isothermal a priori profile was adopted. This bifurcated feature is absent from similar tests of quiescent longitudes in the same latitude band, which demonstrates that it is indeed associated with the auroral hot spots alone. There is no sensitivity of the H_2 S(1) and CH_4 emission spectra to pressures lower than 10 μbar, and so retrieved profiles tend back to the a priori profile in this range and therefore exhibit significant variation depending on the chosen a priori. We discuss the possible sources of 1 mbar heating in section 5 in the context of the observed variability of temperatures from December 2014 to April 2016.

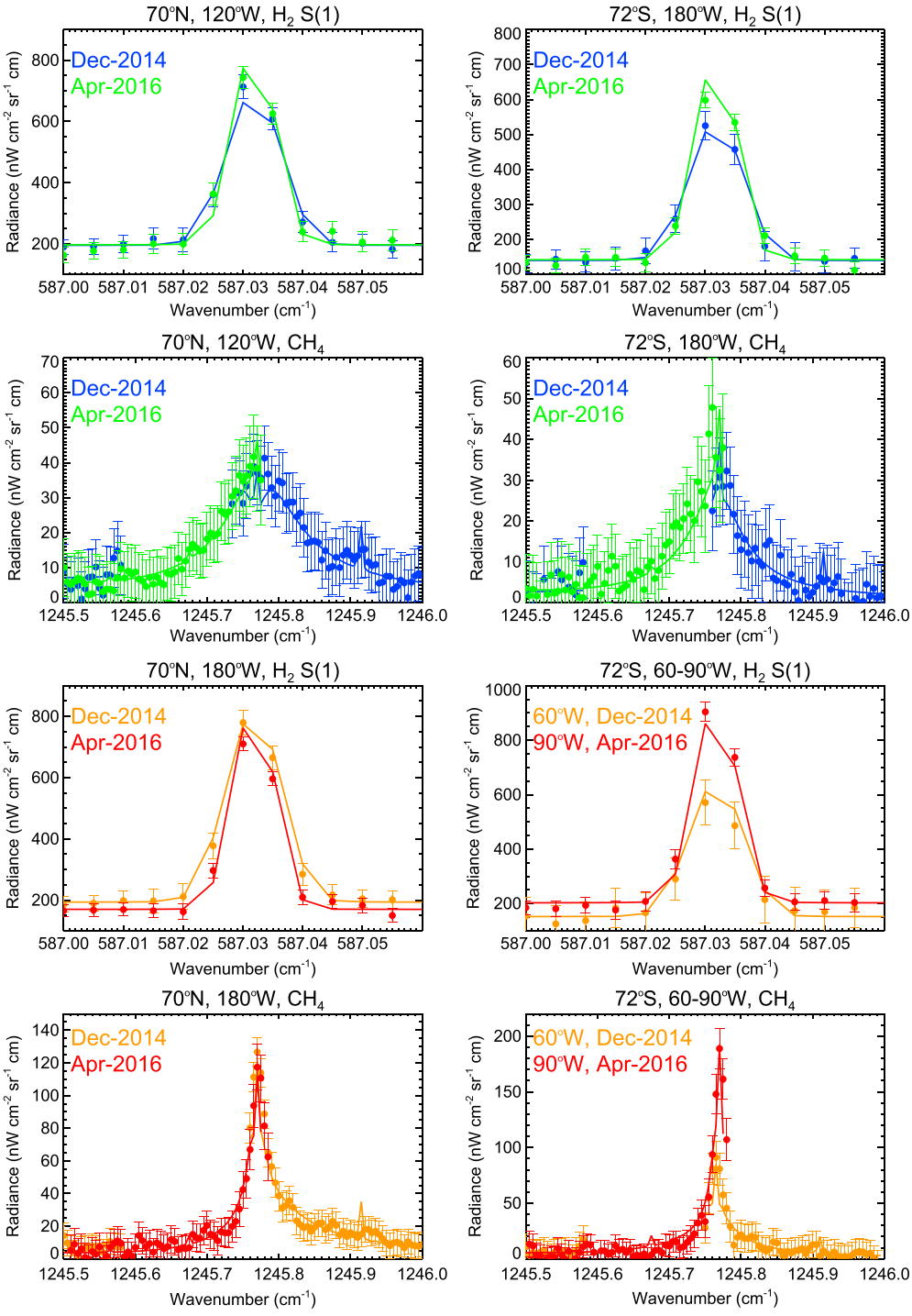

Figure 3. Comparisons of observed (points with error bars) and modelled (solid lines) spectra of the H_2 S(1) and CH_4 emission features in a northern quiescent location (left column, first and second panels) and southern quiescent location (right column, first and second panels) with blue indicating spectra in December 2014 and green indicating spectra in April 2016. Similarly, observed and modelled spectra are compared for the northern auroral hot spot (left column, third and fourth panels) and the southern auroral hot spot (right column, third and fourth panels). Readers should note that H_2 S(1) spectra were obtained at a resolution of 0.0078 cm^{-1} in April 2016 but at a resolution of 0.012 cm^{-1} in December 2014. Only a subset of the CH_4 emission features that were measured and modelled are shown for clarity. In the southern auroral hot spot, we compare 72°S, 60°W in December 2014 and 72°S, 90°W in April 2016, which mark the locations of the warmest 1 mbar temperature associated with the southern auroral hot spot as we believe that it rotated in longitude between 2014 and 2016. The modelled spectra shown correspond to the a priori profile that yielded the best fit to the observations in Figure 2.

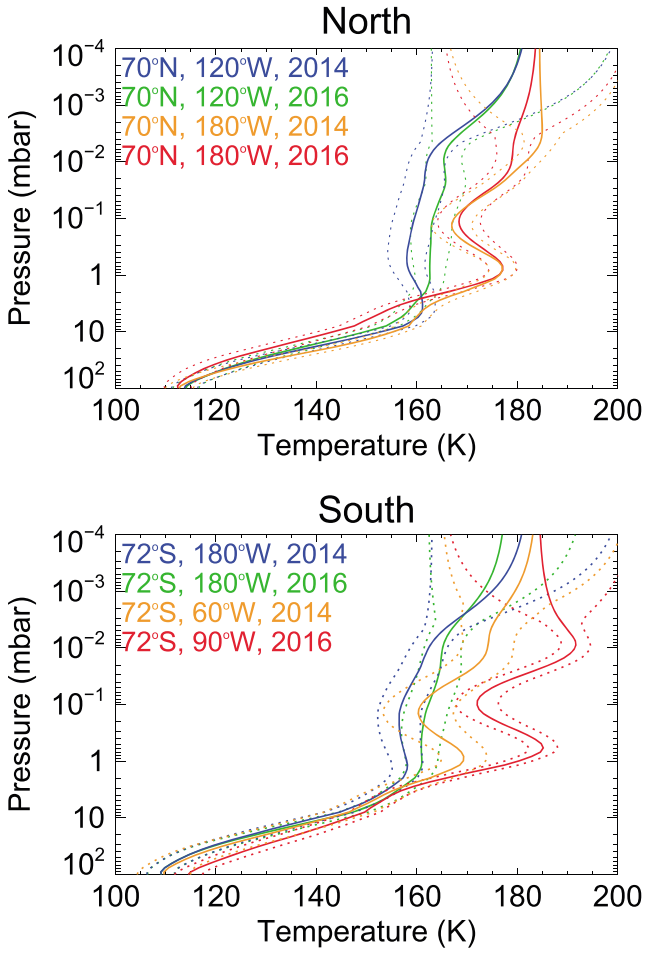

Figure 4. Retrieved vertical temperature profiles (solid lines) at 70°N, 120°W (a representative quiescent location); 70°N, 180°W (the northern auroral hot spot); 72°S 180°W (a quiescent location in the south); and 72°S, 60°W/90°W (the southern auroral hot spot). Results in December 2014 and April 2016 are shown in colors according to the legend provided. The uncertainty on the retrieved profiles (dotted lines) was set to be the largest of the 1σ retrieval error or the variation in retrieved values due to the choice of a priori.

4. Evolution From December 2014 to April 2016

December 2014 and April 2016 measurements are compared in order to deduce the evolution of temperatures over this time range. As conducted for the April 2016 measurements in Figure 2, further temperature retrievals were performed at 70°N, 120°W; 70°N, 180°W; 72°S, 60°W; and 72°S, 180°W starting from different a priori profiles to test the robustness of retrieved parameters. At each location, mean temperature profile and uncertainty were calculated from the temperature profiles retrieved from different a priori and the uncertainty on this mean was assumed to be the larger of either (1) the errors combined in quadrature or (2) the standard deviation on the mean. Equations (1)–(3) in *Sinclair et al.* [2017] provide further details of these calculations. Figure 3 compared the observed and modelled spectra, which yielded the best fit, and Figure 4 compares the mean vertical temperature profiles in December 2014 and April 2016 and uncertainties in all four locations.

Temperatures in the northern auroral hot spot at 1 mbar and 10 μbar exhibit negligible net change of 0.1 ± 3.7 K and −2.5 ± 4.4 K, respectively. In addition, the longitudinal position of the warmest temperatures associated with the northern auroral hot spot appears fixed in position at 70°N, 180°W. However, there is an obvious increase in stratospheric temperatures at high southern latitudes. In comparing temperatures at 72°, 60°W in December 2014 and 72°S, 90°W in April 2016, which represent the longitudes with the highest retrieved temperatures, we derive a net increase in temperature of 11.1 ± 5.2 K at 1 mbar and 17.3 ± 6.0 K at 10 μbar. The lack of a similar temperature increase at 180°W (a quiescent longitude) in the same latitude band indicates that this temperature change cannot be a radiometric calibration inconsistency. While gaps in spatial coverage prevent a direct comparison of temperatures in December 2014 and April 2016 at some longitudes, the orientation of the southern auroral stratospheric heating appears to have rotated approximately 30°in longitude, as has been observed previously [*Caldwell et al.*, 1988].

5. Discussion

Measurements in December 2014 and April 2016 indicate that stratospheric temperatures in the northern and southern auroral regions exhibited different variability over the same timescale. The derived variability of 1 mbar and 10 μbar temperatures on the order of 10 to 20 K has been observed previously on daily timescales in measurements of Jupiter's northern auroral C_2H_6 and C_2H_4 emission [*Livengood et al.*, 1993; *Romani et al.*, 2008]. *Sinclair et al.* [2017] suggested the following mechanisms as the source of 1 mbar heating in auroral regions: (1) absorption of shortwave radiation by haze particles produced by the auroral chemistry

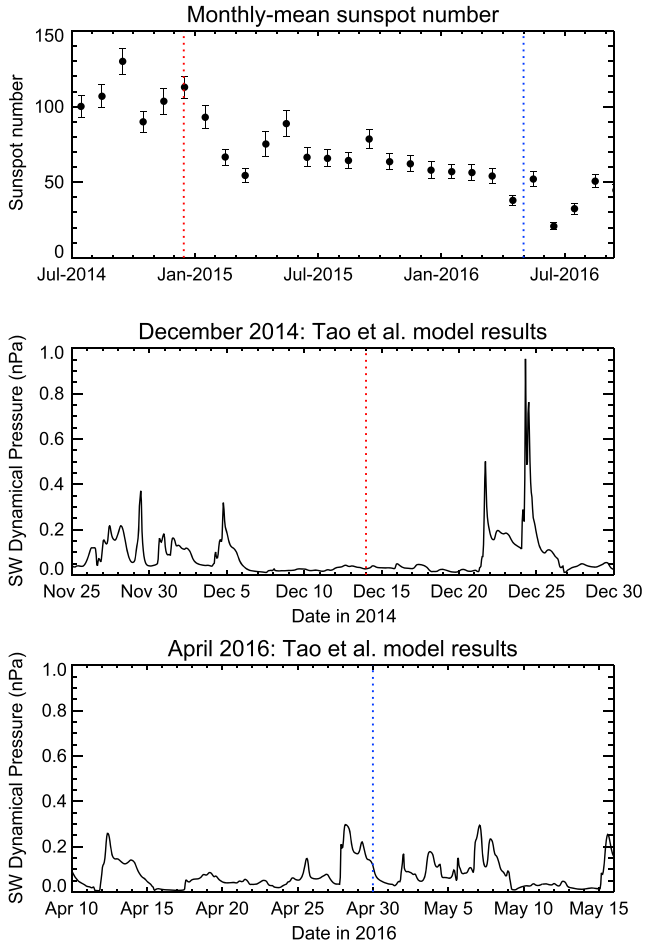

Figure 5. (top) The observed monthly mean and standard deviation of the sunspot number (points with error bars) from 2014 to 2016 (taken from https://solarscience.msfc.nasa.gov/greenwch/SN_m_tot_V2.0.txt) as a measure of the longer-term solar variability associated with its 11 year cycle. (middle and bottom) Solar wind propagation model results of the solar wind dynamical pressures at Jupiter [*Tao et al.*, 2005, 2016] within a month of the TEXES measurements in December 2014 and April 2016 (respectively shown as red and blue vertical dashed lines).

and/or (2) precipitation of a high-energy population of charged particles. We discuss each of these hypotheses below in the context of the variability indicated by the TEXES results.

5.1. Heating By Auroral Haze Particles

The injection of charged particles into Jupiter's upper atmosphere greatly increases the rates of ion neutral chemical reactions in auroral regions with respect to quiescent longitudes. This increases the production of polycyclic aromatic hydrocarbons, which form the building blocks of haze particles [*Wong et al.*, 2000, 2003; *Zhang et al.*, 2015], which have been observed as dark features in ultraviolet observations by Cassini [*West et al.*, 2003]. From December 2014 to April 2016, we note that the subsolar latitude on Jupiter moved from 0.3°N to 2.4°S. Thus, the southern auroral region experienced an increase in solar insolation, while the northern auroral region experienced a decrease. If there are indeed haze particles in the auroral regions, a heating would be expected in the southern auroral region and a cooling would be expected in the northern auroral region. However, assuming that such haze particles are in radiative equilibrium, the increase in their effective temperature as a result of the lower solar zenith angle can only explain up to approximately 2 K of the 11.1 ± 5.2 K 1 mbar temperature change in the southern auroral region. Thus, radiative forcing of the auroral haze particles alone cannot explain the observed temperature change.

5.2. High-Energy Particle Precipitation

Independent variability of X-ray, ultraviolet, and near-infrared H_3^+ auroral emission, which highlight the precipitation of energetic particles into Jupiter's atmosphere, have also been observed. Observations of auroral X-ray emission measured in 2007 and May–July 2016 by Chandra and X-ray Multi Mirror Mission-Newton reveal that the southern and northern auroral regions exhibit uncorrelated variability between observations [*Dunn et al.*, 2016]. Similarly, ultraviolet observations measured by Juno's UVS instrument during orbital insertion of the spacecraft in July 2016 indicated that the southern auroral region brightened independently of the northern auroral region [*Gladstone et al.*, 2016, 2017 (this issue)]. Near-infrared H_3^+ measurements made by Juno's JIRAM instrument during the first perijove in late August 2016 also highlighted that auroral emission from the southern auroral region was approximately 25% brighter compared to the north [*Adriani et al.*, 2016, 2017 (this issue)].

With temperature distributions retrieved on only two dates separated by 17 months, it cannot be concluded whether the variability in 1 mbar temperature in the southern auroral region is a result of a rapid variability (on daily timescales) or a slowly evolving change. Nevertheless, the increase in stratospheric temperatures

in the southern auroral region at times when the ultraviolet and near-infrared southern auroral emission was observed to brighten independently of the north is suggestive of a correlation. The ultraviolet brightening of the southern auroral region during orbital insertion was sometimes found to be correlated to increases in the solar wind dynamical pressure at Jupiter [*Gladstone et al.*, 2016]. In order to assess the potential correlation of the southern auroral ultraviolet and near-infrared brightening with 1 mbar temperature increase, we investigated the longer-term solar variability and the variability of the local solar wind conditions at Jupiter over December 2014 to April 2016 time range (Figure 5).

Over this time range, the monthly mean sunspot number decreased by over a factor of 2. Using a long-term record of measurements from 1979 to 2016, *Kostiuk et al.* [2016] concluded that the strongest C_2H_6 emission (as a probe of temperature) in the northern auroral region occurred during periods of higher solar activity. Although not significant with respect to uncertainty, our results do indicate a cooling near the northern auroral region during a period of decreasing solar activity, which is consistent with the conclusions of *Kostiuk et al.* [2016]. In contrast, we have ruled out such a relationship of 1 mbar temperature in the southern auroral region with this longer-term solar activity since we derived a temperature increase of greater than 10 K when the monthly mean sunspot number decreased by a factor of 2. In order to explain the southern auroral 1 mbar temperature increase, we look instead to the short-term variability of the local solar wind conditions at Jupiter. As shown in Figure 5, downstream solar wind conditions at Jupiter were quiescent in ~8 days preceding the TEXES measurements in December 2014. However, TEXES measurements in April 2016 were acquired within 3 days of a solar wind compression event where the dynamical pressure increased by approximately a factor of 3. This might imply that the southern auroral 1 mbar temperature increase was driven by an increase in the flux of charged particles impinging on the atmosphere of Jupiter. This would require precipitation of charged particles with energies significantly higher than 300 keV [*Kim*, 1988], which have been observed in the Jovian radiation belt [*Bolton et al.*, 2002]. The fact that the vertical temperature profile is bifurcated at 1 mbar and 10 μbar levels might represent the precipitation of two discrete energy populations of charged particles. This hypothesis will be tested in future work using auroral precipitation models.

The shift in longitudinal orientation of warm stratospheric temperatures associated with the southern auroral region between December 2014 and April 2016 has been observed previously [e.g., *Caldwell et al.*, 1988]. The cause of this still remains uncertain. Again, we cannot say whether this change in position is a slowly evolving change over this time range or a snapshot of much more rapid variability. However, the position of the southern auroral oval in X-ray, ultraviolet, and near-infrared H_3^+ emission was observed to be persistent in longitude in 2016 [*Dunn et al.*, 2016; *Nichols et al.*, 2016]. Further observations, obtained at a higher temporal cadence, are required to establish how and why the orientation of southern auroral heating moves in longitude and to test the hypotheses that 1 mbar stratospheric temperatures in the southern auroral region vary according to the solar wind dynamical pressure.

6. Conclusions

Retrievals of temperature from IRTF-TEXES spectra measured in December 2014 and April 2016 reveal that the thermal structures in Jupiter's northern (70°N, 180°W) and southern auroral regions (72°S, 50–80°W) have evolved differently. At 1 mbar, temperatures in the northern auroral region remained constant within uncertainty while temperatures in the southern auroral region exhibited a net increase of ~11.1 ± 5.2 K. This temperature increase occurs over a period of decreasing monthly mean sunspot number and so does not appear to be related to the ~11 year solar cycle. We instead suggest this stratospheric warming of the southern auroral region to be linked to a brightening of the near-infrared and ultraviolet southern auroral emission resulting from short-term increases in the solar wind dynamic pressure at Jupiter. From the results of a solar wind propagation model, TEXES measurements in April 2016 were acquired within 3 days of a solar wind compression event whereas TEXES measurements in December 2014 were acquired after 8 days of quiescent solar wind conditions. The variability of stratospheric temperatures in the auroral region on these short timescales and its apparent time proximity with the solar wind dynamical pressure would favor the precipitation of a high-energy population of charged particles as an explanation of 1 mbar auroral-related heating. Further observations acquired with shorter time separations are required to confirm this hypothesis.

Acknowledgments
In accordance with AGU's data policy, all data presented in this work can be obtained from the primary author (J.S., e-mail: james.sinclair@jpl.nasa.gov). Many thanks are due to the Infrared Telescope Facility, which is operated by the University of Hawaii under contract NNH14CK55B with the National Aeronautics and Space Administration. Many thanks to the NASA Postdoctoral Program, managed by Oak Ridge Associated Universities and Universities Space Research Administration, for funding and supporting Sinclair during this research. Orton was supported by grants from NASA to Jet Propulsion Laboratory/California Institute of Technology. Fletcher was supported by a Royal Society Fellowship at the University of Leicester, and remaining UK authors thank the Science and Technology Facilities Council for their support.

References

Adriani, A., et al. (2016), An overview of the Juno JIRAM results from the first perijove pass, Abstract U22A-02 presented at 2016 Fall Meeting, AGU, San Francisco, Calif., 11–15 Dec.

Adriani, A., et al. (2017), Preliminary JIRAM results from Juno polar observations: 2. Analysis of the Jupiter southern H3+ emissions and comparison with the north aurora, *Geophys. Res. Lett.*, *44*, doi:10.1002/2017GL072905.

Bolton, S., and Juno Science Team (2006), The Juno new frontiers Jupiter polar orbiter mission, paper presented at 2006 European Planetary Science Congress, p. 535, Berlin, Germany, 18–22 Sept.

Bolton, S., and J. S. Team (2016), Early results from the Juno mission at Jupiter, paper presented at AAS/Division for Planetary Sciences Meeting Abstracts vol. 48, p. 316.01.

Bolton, S. J., et al. (2002), Ultra-relativistic electrons in Jupiter's radiation belts, *Nature*, *415*, 987–991, doi:10.1038/415987a.

Bonfond, B., D. Grodent, J.-C. Gérard, T. Stallard, J. T. Clarke, M. Yoneda, A. Radioti, and J. Gustin (2012), Auroral evidence of Io's control over the magnetosphere of Jupiter, *Geophys. Res. Lett.*, *39*, L01105, doi:10.1029/2011GL050253.

Caldwell, J., F. C. Gillett, and A. T. Tokunaga (1980), Possible infrared aurorae on Jupiter, *Icarus*, *44*, 667–675, doi:10.1016/0019-1035(80)90135-9.

Caldwell, J., R. Halthore, G. Orton, and J. Bergstralh (1988), Infrared polar brightenings on Jupiter. IV—Spatial properties of methane emission, *Icarus*, *74*, 331–339, doi:10.1016/0019-1035(88)90045-0.

Drossart, P., B. Bezard, S. Atreya, J. Lacy, and E. Serabyn (1986), Enhanced acetylene emission near the north pole of Jupiter, *Icarus*, *66*, 610–618, doi:10.1016/0019-1035(86)90094-1.

Drossart, P., B. Bezard, S. K. Atreya, J. Bishop, J. H. Waite Jr., and D. Boice (1993), Thermal profiles in the auroral regions of Jupiter, *J. Geophys. Res.*, *98*, 18,803–18,811, doi:10.1029/93JE01801.

Dunn, W. R., et al. (2016), Jupiter's X-ray aurora during the Juno approach, in *RAS Specialist Discussion Meeting—Multi-Scale Dynamics*.

Flasar, F. M., et al. (2004a), An intense stratospheric jet on Jupiter, *Nature*, *427*, 132–135.

Flasar, F. M., V. G. Kunde, M. M. Abbas, R. K. Achterberg, P. Ade, A. Barucci, B. Bézard, G. L. Bjoraker, J. C. Brasunas, and S. Calcutt (2004b), Exploring the Saturn system in the thermal infrared: The composite infrared spectrometer, *Space Sci. Rev.*, *115*(1–4), 169–297.

Friedson, A. J., A.-S. Wong, and Y. L. Yung (2002), Models for polar haze formation in Jupiter's stratosphere, *Icarus*, *158*, 389–400, doi:10.1006/icar.2002.6885.

Giles, R. S., L. N. Fletcher, P. G. J. Irwin, H. Melin, and T. S. Stallard (2016), Detection of H_3^+ auroral emission in Jupiter's 5-micron window, *Astron. Astrophys.*, *589*, A67, doi:10.1051/0004-6361/201628170.

Gladstone, G. R., et al. (2002), A pulsating auroral X-ray hot spot on Jupiter, *Nature*, *415*, 1000–1003.

Gladstone, R., et al. (2016), Initial observations of Jupiter's aurora from Juno's Ultraviolet Spectrograph (Juno-UVS) (Invited), Abstract U22A-01 presented at 2016 Fall Meeting, AGU, San Francisco, Calif., 11–15 Dec.

Gladstone, R., et al. (2017), Juno-UVS Approach Observations of Jupiter's Auroras, *Geophys. Res. Lett.*, *44*, doi:10.1002/2017GL073377.

Irwin, P. G. J., N. A. Teanby, R. de Kok, L. N. Fletcher, C. J. A. Howett, C. C. C. Tsang, C. F. Wilson, S. B. Calcutt, C. A. Nixon, and P. D. Parrish (2008), The NEMESIS planetary atmosphere radiative transfer and retrieval tool, *J. Quant. Spectrosc. Radiat. Transfer*, *109*, 1136–1150.

Kim, S. J. (1988), Infrared processes in the Jovian auroral zone, *Icarus*, *75*, 399–408, doi:10.1016/0019-1035(88)90153-4.

Kim, S. J., J. Caldwell, A. R. Rivolo, R. Wagener, and G. S. Orton (1985), Infrared polar brightening on Jupiter. III—Spectrometry from the Voyager 1 IRIS experiment, *Icarus*, *64*, 233–248, doi:10.1016/0019-1035(85)90088-0.

Kostiuk, T., P. Romani, F. Espenak, and T. A. Livengood (1993), Temperature and abundances in the Jovian auroral stratosphere. 2: Ethylene as a probe of the microbar region, *J. Geophys. Res.*, *98*, 18,823–18,830, doi:10.1029/93JE01332.

Kostiuk, T., T. A. Livengood, T. Hewagama, K. E. Fast, G. L. Bjoraker, F. Schmuelling, S. Guido, and J. R. Kolasinski (2016), Variability of mid-infrared aurora on Jupiter: 1979 to 2016, in American Geophysical Union Fall Meeting 2016, Abstract P33C-2155 presented at 2016 Fall Meeting, AGU, San Francisco, Calif., 11–15 Dec.

Lacy, J. H., M. J. Richter, T. K. Greathouse, D. T. Jaffe, and Q. Zhu (2002), TEXES: A sensitive high-resolution grating spectrograph for the mid-infrared, *Publ. Astron. Soc. Pac.*, *114*, 153–168, doi:10.1086/338730.

Livengood, T. A., T. Kostiuk, and F. Espenak (1993), Temperature and abundances in the Jovian auroral stratosphere. 1: Ethane as a probe of the millibar region, *J. Geophys. Res.*, *98*, 18,813–18,821, doi:10.1029/93JE01043.

Moses, J. I., T. Fouchet, B. Bézard, G. R. Gladstone, E. Lellouch, and H. Feuchtgruber (2005), Photochemistry and diffusion in Jupiter's stratosphere: Constraints from ISO observations and comparisons with other giant planets, *J. Geophys. Res.*, *110*, E08001, doi:10.1029/2005JE002411.

Nichols, J. D., E. J. Bunce, J. T. Clarke, S. W. H. Cowley, J.-C. Gérard, D. Grodent, and W. R. Pryor (2007), Response of Jupiter's UV auroras to interplanetary conditions as observed by the Hubble Space Telescope during the Cassini flyby campaign, *J. Geophys. Res.*, *112*, A02203, doi:10.1029/2006JA012005.

Nichols, J. D., et al. (2016), Jupiter's auroras during the Juno approach phase as observed by the Hubble Space Telescope, Abstract P24B-01 presented at 2016 Fall Meeting, AGU, San Francisco, Calif., 11–15 Dec.

Ozak, N., D. R. Schultz, T. E. Cravens, V. Kharchenko, and Y.-W. Hui (2010), Auroral X-ray emission at Jupiter: Depth effects, *J. Geophys. Res*, *115*, A11306, doi:10.1029/2010JA015635.

Romani, P. N., D. E. Jennings, G. L. Bjoraker, P. V. Sada, G. H. McCabe, and R. J. Boyle (2008), Temporally varying ethylene emission on Jupiter, *Icarus*, *198*, 420–434, doi:10.1016/j.icarus.2008.05.027.

Sinclair, J. A., G. S. Orton, T. K. Greathouse, L. N. Fletcher, J. I. Moses, V. Hue, and P. G. J. Irwin (2017), Jupiter's auroral-related stratospheric heating and chemistry. I: Analysis of Voyager-IRIS and Cassini-CIRS spectra, *Icarus*, *292*, 182–207, doi:10.1016/j.icarus.2016.12.033.

Stallard, T. S., A. Masters, S. Miller, H. Melin, E. J. Bunce, C. S. Arridge, N. Achilleos, M. K. Dougherty, and S. W. H. Cowley (2012), Saturn's auroral/polar H_3^+ infrared emission: The effect of solar wind compression, *J. Geophys. Res.*, *117*, A12302, doi:10.1029/2012JA018201.

Tao, C., R. Kataoka, H. Fukunishi, Y. Takahashi, and T. Yokoyama (2005), Magnetic field variations in the Jovian magnetotail induced by solar wind dynamic pressure enhancements, *J. Geophys. Res.*, *110*, A11208, doi:10.1029/2004JA010959.

Tao, C., T. Kimura, F. Tsuchiya, G. Murakami, K. Yoshioka, H. Kita, A. Yamazaki, Y. Kasaba, I. Yoshikawa, and M. Fujimoto (2016), Jupiter's Auroral Energy Input Observed by Hisaki/EXCEED and Its Modulations by Io's Volcanic Activity, Abstract P33C-2151 presented at 2016 Fall Meeting, AGU, San Francisco, Calif., 11–15 Dec.

West, R. A., D. Griswold, and C. Porco (2003), Jupiter's Polar UV Great Dark Spot, paper presented at AAS/Division for Planetary Sciences Meeting Abstracts, vol. 35, p. 1009, Bull. of the Am. Astron. Soc.

Wong, A.-S., A. Y. T. Lee, Y. L. Yung, and J. M. Ajello (2000), Jupiter: Aerosol chemistry in the polar atmosphere, *Astrophys. J. Lett.*, *534*, L215–L217, doi:10.1086/312675.

Wong, A.-S., Y. L. Yung, and A. J. Friedson (2003), Benzene and haze formation in the polar atmosphere of Jupiter, *Geophys. Res. Lett.*, *30*(8), 1447, doi:10.1029/2002GL016661.

Zhang, X., R. A. West, P. G. J. Irwin, C. A. Nixon, and Y. L. Yung (2015), Aerosol influence on energy balance of the middle atmosphere of Jupiter, *Nat. Commun.*, *6*, 10231, doi:10.1038/ncomms10231.